Supplementary Material

Expression of specific inflammasome gene modules stratifies older individuals into two extreme clinical and immunological states

David Furman[1,2*], Junlei Chang[3], Lydia Lartigue[4], Christopher R Bolen[5¶], François Haddad[6], Brice Gaudilliere[5], Edward A. Ganio[5], Gabriela K. Fragiadakis[5], Matthew H. Spitzer[5], Isabelle Douchet[7], Sophie Daburon[7], Jean-François Moreau[7], Garry P. Nolan[5], Patrick Blanco[7], Julie Déchanet-Merville[7], Cornelia L Dekker[8], Vladimir Jojic[9], Calvin J Kuo[3], Mark M Davis[1,10*], Benjamin Faustin[7*]

[1]*Institute for Immunity, Transplantation and Infection, Stanford University School of Medicine, 279 Campus Drive, Beckman Center, 94305, Stanford, California, USA*
[2]*Department of Systems Biology, Division of Translational Medicine, Sidra Medical and Research Center, Al Luqta Street, Education City North Campus, PO Box 26999, Doha, Qatar*
[3]*Department of Medicine, Division of Hematology, Stanford University School of Medicine, 265 Campus Drive, Lokey Stem Cell Research Building G2045, 94305, Stanford, California, USA*
[4]*INSERM U916 VINCO, Institut Bergonié, 229 cours de l'Argonne, 33076 Bordeaux Cedex, France*
[5]*Department of Microbiology and Immunology, Stanford University School of Medicine, 269 Campus Drive, CCSR Building, 94305, Stanford, California, USA*
[6]*Institute of Cardiovascular Medicine, Stanford University School of Medicine, 279 Campus Drive, Beckman Center, 94305, Stanford, California, USA*
[7]*CIRID, UMR CNRS 5164, Université Bordeaux 2, 146 rue Léo Saignat, 33076 Bordeaux Cedex, France*
[8]*Department of Pediatrics, Division of Infectious Diseases, Stanford University, Stanford, California, 94305, USA*
[9]*Department of Computer Science, University of North Carolina, Chapel Hill, North Carolina, 27599, USA*
[10]*Howard Hughes Medical Institute, Stanford University School of Medicine, 279 Campus Drive, Beckman Center, 94305, Stanford, California, USA*
¶Current address: Bioinformatics Department, Genentech Inc., 1 DNA Way Mailstop 258A, 94080, South San Francisco, California, USA

Nature Medicine: doi:10.1038/nm.4267

2. Supplementary Methods

Gene expression analysis

Two different microarray platforms were used to generate expression data from whole blood samples obtained from a total of 114 individuals recruited as part of the Stanford-Ellison longitudinal cohort[1-3]; the Human HT12v3 Expression Bead Chip (Illumina, San Diego, CA) for years 2008 and 2009, and the GeneChip PrimeView Human Gene Expression Array (Affymetrix, Santa Clara, CA), for years 2010, 2011 and 2012. For this study, we did not pre-specify effect size, however, based on our previous studies on these same cohorts, we estimated that 114 individuals would provide a statistical power of 0.75 ($\alpha = 0.05$) for an effect size of 0.3. For the Illumina platform, biotinylated, amplified antisense complementary RNA (cRNA) targets were prepared from 200 to 250 ng of the total RNA using the Illumina RNA amplification kit (Applied Biosystems/Ambion). Seven hundred and fifty nanograms of labeled cRNA was hybridized overnight to Illumina Human HT-12v3 BeadChip arrays (Illumina), which contained >48,000 probes. The arrays were then washed, blocked, stained and scanned on an Illumina BeadStation 500 following the manufacturer's protocols. BeadStudio/GenomeStudio software (Illumina) was used to generate signal intensity values from the scans. For normalization, the software was used to subtract background and scale average signal intensity for each sample to the global average signal intensity for all samples. A gene expression analysis software program, GeneSpring GX version 7.3.1 (Agilent Technologies), was used to perform further normalization under the default percentile shift settings. During this process the signal values are transformed to the log base, then the log transformed signal values are arranged in increasing order and the rank of the required percentile (Pth) is

Nature Medicine: doi:10.1038/nm.4267

computed. Once the value corresponding to the Pth percentile is obtained, this value is subtracted from the corresponding log transformed signal values and this gives the normalized intensity value. For the Affymetrix platform standard Affymetrix 3'IVT Express protocol was used to generate biotinylated cRNA from 50-500 ng of total RNA. DNA polymerase was used for the production of double stranded cDNA. T7 RNA polymerase, in the presence of biotinylated nucleotides, was used for *in vitro* transcription (IVT) of biotinylated cRNA. The fragmented and labeled targets were hybridized to the PrimeView Human Gene Expression Array cartridge, which measure gene expression of more than 36,000 transcripts and variants per sample by using multiple (11 probes per set for well-annotated sequences, 9 probes per set for the remainder) independent measurements for each transcript. The standard Affymetrix hybridization protocol includes 16hr (overnight) hybridization at 45 degree at 60rpm in an Affymetrix GeneChip Hybridization Oven 645. The arrays were then washed and stained in an Affymetrix GeneChip Fluidics Station 450. The arrays were scanned using the Affymetrix GeneChip Scanner 3000 7G and the Affymetrix GeneChip Command Console Software (AGCC) was used for the gene expression data processing and extraction. The raw data for years 2008 through 2012 has been deposited on the Immunology Database and Analysis Portal (ImmPort, https://immport.niaid.nih.gov) under accession numbers SDY314, SDY312, SDY311, SDY112 and SDY315, respectively.

To identify gene modules associated with IL-1β production and inflammasome activity, a list of a total of 89 genes including the Pattern-Recognition Receptor family and their positive and negative regulators encompassing TLRs, NLRs, RIG-I-Like Receptors

Nature Medicine: doi:10.1038/nm.4267

(RLRs), C-type lectin-like Receptors (CLRs) and their adaptors; inflammatory caspases and their direct regulators; and transcription factors involved in NF-kB and Type-I Interferon (IFN) signaling which are known to regulate inflammasome gene expression and activation was gathered from manually curated data. We searched for the presence of these genes across a total of 109 previously defined gene modules[2]. A gene module corresponds to a set of co-expressed genes sharing regulatory programs[4,5]. Briefly, data were filtered by variance and a total of 6234 highly variant genes (standard deviation cutoff = 0.24) were normalized by centering and scaling the expression so that each gene's expression across all subjects had euclidean norm equal to 1 for purposes of clustering. Data was log transformed to approximate to normal distribution. We utilized hierarchical agglomerative clustering with average linkage, euclidean distance and a height cutoff value of 1.5 to derive 109 modules. For each gene module, we assigned a set of regulatory genes (regulatory program), based on regression analysis of genes in the modules onto expression of known transcription factors using a Akaike Information Criterion (AIC)[6]. To do so, we performed linear regression with elastic net penalty of each module's expression onto a set of 188 transcription factors using LARS-EN algorithm. To select the best model among the outputs of LARS-EN, we assessed quality of the resulting models by AIC, with sample specific terms weighted by within-module variance. The fit with the best AIC score was selected for each module. For all 109 gene modules, annotation was computed based on Gene Set Enrichment Analysis[7]. For accessing the gene modules, regulatory programs and annotations see http://cs.unc.edu/~vjojic/fluy2-upd/.

Nature Medicine: doi:10.1038/nm.4267

To determine the stability of the age-associations for module 62 and 78, we used the QuSAGE gene set analysis method[8], which creates a probability distribution representing the mean and standard deviation of a set of genes and enables comparisons of gene sets across different groups. For this analysis, samples from the individuals' first appearance in the study were used to analyze the age associations for module expression.

We examined the presence of extreme phenotypes by using classification based on the magnitude and stability (chronicity) of the expression levels. For each year, the expression of modules 62 and 78 were used to bin subjects into quartiles. Subjects were assigned into inflammasome module high (IMH) or inflammasome module low (IML) groups if they were in the upper (top 25% of subjects) or lower quartile (bottom 25%) in at least in 3/5 years, respectively. Subjects who were not in the upper or lower quartiles in at least 3/5 years were not included in this analysis.

Estimation of cell frequency using gene expression analysis

We estimated the frequencies of 22 different cell subsets in IMH and IML older adults (N = 22), and in a separate analysis, we compared such frequencies between young and older adults (N = 86). For these analyses we used Cibersort[9], which uses gene expression profiles to characterize cell subset composition in complex tissues, such as whole blood. We found significant differences in the estimated frequencies of circulating mast cells, as well as in the CD4 T regulatory cell compartment between young and older adults (P < 0.01). However, no significant differences were observed for any of the other cell subsets analyzed. Similarly, there were no significant differences in cell subset frequencies between IMH and IML older adults (Fig. S7).

Nature Medicine: doi:10.1038/nm.4267

Mass cytometry (CyTOF)

Antibodies

Antibodies were either obtained pre-conjugated from the manufacturer (Fluidigm, South San Francisco, CA) or were conjugated in-house to the appropriate metal isotopes (Table S5). Purified unconjugated antibodies in carrier-protein-free PBS were labeled using the MaxPAR antibody conjugation kit (Fluidigm) using the manufacturer's protocol. Conjugated antibodies were stored at a concentration of 0.2mg/mL (based on percent yield calculated from measured absorbance at 280nm) in Candor PBS Antibody Stabilization solution (Candor Biosciences, Wangen, Germany) at 4°C. Antibodies were titrated on whole blood and used at concentrations listed in Supplementary Table 6.

Sample thaw and red blood cell lysis

Fixed samples were thawed for 10 minutes at 4°C and 10 minutes in a room temperature water bath. Samples were filtered using a 100μm membrane into a hypotonic lysis solution (Smart tube Inc., San Carlos, CA) and incubated for 5 minutes at room temperature. Samples were centrifuged and resuspended in lysis solution for 5 minutes and washed twice with cell-staining media (CSM, phosphate buffered saline with 0.5% bovine serum albumin, 0.02% NaN_3).

Mass-tag cellular barcoding

To minimize experimental variability, samples were barcoded as previously described. Briefly, Isothiocyanobenzyl-EDTA/Pd (Pd)-based reagents were prepared for mass tag

Nature Medicine: doi:10.1038/nm.4267

barcoding as described[10-12]. Twenty-well barcode plates were prepared, each well containing a unique combination of three Pd isotopes (102, 104, 105, 106, 108, 110) at 200nM in DMSO. After sample thaw and red blood cell lysis, cells were washed with once with CSM, once with PBS, and once with 0.02% Saponin in PBS. Barcoding plates were thawed and resuspended in 1ml 0.02% Saponin in PBS. Barcoding reagent was added to each sample and incubated shaking at room temperature for 15 minutes. Samples were subsequently washed twice with CSM and pooled into a single tube for antibody staining. Samples were run on three barcode plates; to facilitate comparisons, all samples from a feto-maternal pair run on the same barcode plate.

Antibody staining

Pooled barcoded samples were incubated with a cocktail of antibodies against surface antigens (Supplementary Table 6) for 30 minutes shaking at room temperature. Samples were washed with CSM, permeabilized with methanol for 10 minutes at 4°C, and washed twice with CSM. Samples were subsequently incubated with a cocktail of antibodies against intracellular proteins (Supplementary Table 6) for 30 minutes shaking at room temperature then washed with CSM. Samples were incubated with an iridium intercalator (Fluidigm) with 1.6% paraformaldehyde in PBS overnight at 4°C.

Mass cytometry measurement

Intercalated samples were washed once with CSM and twice with double distilled water, and resuspended in a solution of normalization beads (Fluidigm). Samples were filtered prior to mass cytometry analysis through a 35μm membrane and analyzed at a flow rate

Nature Medicine: doi:10.1038/nm.4267

of approximately 500 cells/second. Samples were normalized and debarcoded using software described in[12,13].

Statistical tests

Age association of inflammasome gene modules and correlation with clinical outcomes.

For the analysis of age-related gene expression in the Stanford-Ellison longitudinal cohort, we first derived gene modules from microarray data collected during the year 2008. The data were processed as previously described[2]. Briefly, of a total of 48771 gene probes in the microarray per sample, we first selected 6234 based on variance (s.d. cutoff value of 0.24). We then normalized their expression by centering and scaling data so that each gene's expression across all subjects had euclidean norm equal to 1 for purposes of clustering. We conducted hierarchical clustering with average linkage, euclidean distance and a height cutoff value of 1.5 to derive a total of 109 modules. For each gene module a set of regulatory genes were assigned, based on regression analysis of genes in the modules onto expression of transcription factors using a Akaike Information Criterion (AIC; Akaike, 1974). Of a total of 394 transcription factors in total, 188 met the s.d. cutoff value. We performed linear regression with elastic net penalty of each module's expression onto the set of regulators using LARS-EN algorithm with l2 penalty weighted by 0.01. To select the best model among the outputs of LARS-EN, we assessed robustness of the resulting models by AIC. The fit with the best AIC score was selected for each module.

We subsequently searched for gene modules that were correlated with age by the Benjamini-Hochberg method[14], which is based on permutation procedures and outputs a

Nature Medicine: doi:10.1038/nm.4267

false discovery rate (FDR), defined as the expected percentage of false positives among all the claimed positives. Of the 109 gene modules derived from our previous analysis, 41 were correlated with age ($Q \leq 0.05$). We then conducted functional analysis on the age-associated gene modules (totaling 41) by using the DAVID Functional Annotation Bioinformatics Microarray Analysis tool (https://david.ncifcrf.gov/). To validate the findings that modules 62 and 78 were annotated to participate in cytokine production, we conducted hypergeometric tests to identify which sub-populations of gene modules were overrepresented (enriched) for inflammasome genes in our sample. This test uses the hypergeometric distribution to calculate the statistical significance of having drawn a specific k successes (out of n total draws) from the population. Using this analysis we found significant enrichment for these same modules (FDR $Q < 0.01$).

To search for stability of the observed higher expression of inflammasome gene modules in the older cohort, we used the longitudinal data and the expression of these two gene modules in young versus older subjects was compared using the QuSAGE method[8]. For this analysis, samples from the individuals' first appearance in the study ($N = 114$) were used to analyze the age associations for module expression.

When then looked for association with clinical phenotypes. To that end we classified the older cohort into two classes inflammasome module high (IMH) or inflammasome module low (IML) groups if they were in the upper or lower quartiles, respectively, for each gene module in 3 or more of the 5 years analyzed. Subjects who did not meet these criteria were not included in this analysis. For module 62, this yielded 19 individuals with extreme phenotypes: 9 IMH and 10 IML individuals, and for module 78, 16 individuals: 9 IMH and 7 IML. Since the two modules correlated well and a significant degree of

Nature Medicine: doi:10.1038/nm.4267

overlap for the modules 62 and 78 in each category was noted (6 IMH and 6 IML, *P*-value for enrichment < 0.001), IMH (age range 66-86) or IML (age range 62-90) individuals from modules 62 and 78 were combined ($N = 23$) for further analysis.

When then asked whether the IMH vs IML status correlated with clinical phenotypes by logistic regression analysis to compare the IMH and IML phenotypes (N=23) with respect to their clinical history of diabetes, hypertension and psychiatric disorders (all binary outcomes). Because the age range of our older cohorts was relatively large (60 - >89), age and sex were included in the logistic regression models. We also adjusted for other confounding factors such as medication history and body mass index (BMI).

We found a significant association with hypertension but not with other clinical phenotypes.

The analysis of pulse wave velocity (PWV) was done using a two-tail student's *t*-test. The PWV was significantly lower in the IML group (7.9 ± 2.4 m/s) compared to the IMH group (10.7 ± 2.1 m/s) ($P = 0.02$) ($N = 17$, t = -2.4976, df = 13.902).

The analysis of module expression and deaths was also done using two-tail student's *t*-test. For module 62, the p-value was 0.068 (t = -2.0647, df = 9.3161) and for module 78, 0.01 (t = -2.8009, df = 9.8783, p-value = 0.018).

For the analysis of serum cytokines we used data from year 2013 ($N = 16$) an conduced multiple regression analysis on each analyte's MFI against age, sex and IML/IMH status. Significance of the regression coefficients was obtained via permutation tests. For years 2008-2011 the number of samples were as follows: IML (2008, 2009, 2010, 2011) = 10, 10, 8, 7, respectively and IMH (2008, 2009, 2010, 2011) = 12, 11, 12, 8, respectively.

Nature Medicine: doi:10.1038/nm.4267

Metabolomics analysis

The metabolomics analysis was conducted on available serum samples from year 2011 (*N* = 9 IML and 11 IMH). We conducted significance analysis of microarrays (SAM) on a total of 692 metabolites. Sixty-seven were differentially expressed (all upregulated) in IMH versus IML (FDR $Q < 0.2$, score (d) >1.3). Functional annotation and pathway analysis of the metabolites found was conducted using MetPA[33].

We used two-tail student's *t*-test to compare levels of cystine and 8-isoprostane (*N* = 20). The p-value for 8-isoprostane was 0.01 (t = -3.1493, df = 10.087) and the p-value for cystine was 0.018 (t = -2.7667, df = 14.36).

For the stimulation assays using primary monocytes, platelets, granulocytes or THP-1 cells, we either used two or one-tail *t*-test (see Figure legends). Error bars in those cases reflect experimental variability (technical replicates).

Analysis of blood pressure and immune cell activation in mice treated with N4A and adenine

Adult male C57BL/6 mice (12-18-week old) were randomized into either control (*N* = 4 or 10) or treatment (*N* = 4 or 10) groups. The p-value for comparison of blood pressure between the two groups of mice (*N* = 8) was 0.016 (t = -4.4164, df = 4.367). The p-value obtained when comparing the larger set (*N* = 20) was 0.011 (t = -3.0117, df = 11.736).

To analyze the differences in signaling molecules in mice treated with the compunds versus controls (*N* = 12) we used SAM analysis (21 cell surface markers and 10 signaling proteins). The cell subsets analyzed included granulocyes, monocyes, NK cells CD4 and CD8 T cells, T regulatory CD4 T cells and B cells. The panel in the figure 5b shows the

Nature Medicine: doi:10.1038/nm.4267

results of SAM analysis comparing the two groups of mice with the x-axis representing the FDR or significance (at a cutoff of 5%) as a function of score (d) parameter (y-axis), which is equivalent to the *T*-statistic value of a *t*-test when comparing two samples.

Effect of caffeine on inflammasomes

To correlate the levels of caffeine consumption and expression of inflammasome gene modules, we conduced regression on the expression of module 62 and 78 and caffeine consumption in mg/week (adjusted for age, sex and BMI). The caffeine intake levels were estimated from a 15-category survey conducted during the year 2008, derived from 120 of the most commonly consumed caffeinated products in the United States in 2007 (Center for Science in the Public Interest, see http://www.cspinet.org/new/cafchart.htm). The data used in this analysis corresponded to samples collected in the year 2008, $N = 89$).

The differences in circulating caffeine and caffeine metabolites between the IMH and IML groups were computed using one-tail *t*-test and p-values were combined using a modified generalized Fisher method for combining probabilities from dependent tests[15]. Differences in the expression of NLRC4 in THP-1 cells upon treatment with caffeine, N4A and adenine were analyzed by the Student's *t*-test. Figure 6c shows mean ± SD; $N = 3$.

Nature Medicine: doi:10.1038/nm.4267

3. Supplementary Figures and Tables

	2008	2009	2010	2011	2012
Young	29	22	20	28	19
Old	60	51	55	59	52

Supplementary Table 1. Number of young and older subjects per year

Nature Medicine: doi:10.1038/nm.4267

Name	*Mechanism of action*	*Class*
Amlodipine	Calcium channel blocker	1
Atenolol	Beta-blocker	3
Candesatran Cilexetil	Angiotensin II receptor antagonist	2
Carvedilol	Beta-blocker	3
Chlorthalidone	Thiazide diuretic	4
Diltiazem (also XR version)	Calcium channel blocker	1
Doxazosin	Alpha-adrenergic blocker	5
Enalapril	ACE inhibitor	6
Furosemide	Loop diuretic	7
Hydrochlorothiazide (HCTZ)	Thiazide diuretic	4
Lisinopril	ACE inhibitor	6
Lisinopril+HCTZ	ACE inhibitor+thiazide diuretic	6*4
Metoprolol	Beta-blocker	3
Olmesartan	Angiotensin II receptor antagonist	2
Spironolactone	Potassium-sparing diuretic	8
Triamterene	Potassium-sparing diuretic	8
Valsartan	Angiotensin II receptor antagonist	2

Supplementary Table 2. List of medications prescribed in IML and IMH subjects

Nature Medicine: doi:10.1038/nm.4267

analyte	intercept	IMH_IML	Sex	Age
TGFA	0.07153846	0.062	0.744	0.868
NGF	1	0.062	0.744	0.8266667
IL1B	0.07153846	0.1033333	0.93	0.6763636
IL31	0.775	0.1033333	0.93	1
IL23	1	0.1033333	0.5425	1
IFNB	0.07294118	0.155	0.9358491	1
IL17F	1	0.1641176	0.9789474	1
IL21	0.08611111	0.1641176	0.7560976	0.868
SDF1A	0.07294118	0.1653333	0.7294118	1
IL6	1	0.1653333	0.7294118	1
MCSF	0.10333333	0.1653333	0.62	1
FGFB	0.062	0.1653333	0.7294118	1
IL12P70	0.10333333	0.186	0.7294118	1
GROA	0.062	0.186	0.62	1
IFNG	0.093	0.19375	0.7294118	0.6676923
MIG	0.18083333	0.19375	0.744	1
IL13	0.07153846	0.1972727	0.8414286	0.6716667
IL27	0.10333333	0.2066667	0.8266667	1
PIGF1	0.07153846	0.2066667	0.8414286	0.6888889
TRAIL	0.07294118	0.2066667	0.7294118	1
IL1A	0.07153846	0.2066667	0.8414286	0.6888889
TNFA	1	0.2156522	0.744	1
CD40L	1	0.2156522	0.7560976	1
IL8	0.07153846	0.2232	0.62	0.682
MIP1B	1	0.2232	0.7294118	0.7971429
MIP1A	0.07294118	0.2384615	0.8857143	1
TNFB	1	0.2755556	0.9581818	1
IL4	0.12681818	0.2993103	0.9358491	1
GCSF	1	0.2993103	0.7560976	1
IL15	0.093	0.31	0.8266667	1
IL2	1	0.32	0.9789474	1
LIF	1	0.329375	0.8857143	1
FASL	0.07153846	0.3569697	0.7294118	1
IL5	0.2325	0.4536585	1	1
EOTAXIN	0.63589744	0.4536585	0.8857143	1
SCF	0.19076923	0.4536585	1	1
IFNA	0.07153846	0.4536585	0.7560976	1
TGFB	0.22	0.4536585	0.9358491	1
MCP1	0.10333333	0.4536585	0.7294118	1
EGF	0.24424242	0.4536585	0.8266667	1
MCP3	1	0.4536585	0.7560976	1
IL10	1	0.5166667	1	1
IL17A	0.22	0.5166667	0.9789474	1
IL1RA	1	0.5166667	0.744	1
GMCSF	1	0.5166667	0.744	1
VEGFD	0.27352941	0.5166667	0.7560976	1
RESISTIN	0.16173913	0.5166667	0.744	1
VEGF	1	0.5166667	0.8266667	1
BDNF	1	0.5849057	0.6888889	1
IL18	0.22962963	0.5849057	0.8857143	1
VCAM1	0.22	0.5849057	1	1
IL22	1	0.5849057	0.775	1
LEPTIN	1	0.5849057	0.744	1
RANTES	0.90731707	0.6763636	0.5425	1
HGF	1	0.6763636	0.9789474	1
IL7	1	0.7482759	0.9358491	1
IL9	0.19076923	0.7482759	0.5166667	1
PAI1	0.63589744	0.7482759	0.7294118	1
IL12P40	0.63589744	0.8266667	1	1
ICAM1	0.53142857	0.8266667	0.7294118	1
IP10	0.22	0.9147541	0.7294118	1
PDGFBB	0.63589744	1	0.7560976	1

Supplementary Table 3. List of cytokines and chemokines associated with the IMH vs IML groups of older individuals

Nature Medicine: doi:10.1038/nm.4267

Metabolite name	*Score(d)*	*q-value(%)*	*Metabolite name*	*Score(d)*	*q-value(%)*
stachydrine	2.449	0.000	orotidine	1.667	13.780
betonicine	2.429	0.000	xylitol	1.663	13.780
scyllo-inositol	2.362	0.000	N3-methyluridine	1.656	13.780
5,6-dihydrothymine	2.291	0.000	corticosterone	1.652	13.780
N-acetylthreonine	2.272	0.000	pseudouridine	1.644	13.780
N4-acetylcytidine	2.238	0.000	cholate	1.642	13.780
chiro-inositol	2.208	0.000	AICA ribonucleotide	1.636	13.780
vanillylmandelate (VMA)	2.078	0.000	dimethylglycine	1.604	13.780
N6-methyladenosine	2.022	0.000	3-hydroxyhippurate	1.604	13.780
3-hydroxy-3-methylglutarate	2.022	0.000	xanthosine	1.595	13.780
S-adenosylhomocysteine (SAH)	2.004	0.000	N-methylpipecolate	1.583	13.780
acisoga	1.955	0.000	citrate	1.582	13.780
succinylcarnitine	1.939	0.000	hexenedioylcarnitine	1.577	13.780
adenine	1.931	0.000	N-acetylmethionine	1.575	13.780
N6-carbamoylthreonyladenosine	1.884	0.000	quinolinate	1.575	13.780
5,6-dihydrouracil	1.874	0.000	behenoyl sphingomyelin	1.567	13.780
hypotaurine	1.873	13.780	gamma-tocopherol	1.567	13.780
4-acetamidobutanoate	1.852	13.780	N-acetylalanine	1.565	13.780
3-ureidopropionate	1.846	13.780	O-sulfo-L-tyrosine	1.558	13.780
5-methylthioadenosine (MTA)	1.844	13.780	2-aminooctanoate	1.545	13.780
C-glycosyltryptophan	1.825	13.780	xylonate	1.541	13.780
myo-inositol	1.811	13.780	fucitol	1.540	13.780
N-acetylserine	1.778	13.780	3-methoxytyrosine	1.500	15.966
malonate (propanedioate)	1.763	13.780	indolebutyrate	1.495	15.966
N6-acetyllysine	1.760	13.780	17alpha-hydroxypregnanolone glucuronide	1.474	15.966
pyroglutamine	1.725	13.780	3beta,7alpha-dihydroxy-5-cholestenoate	1.473	15.966
homovanillate (HVA)	1.720	13.780	2-hydroxyphenylacetate	1.466	16.880
N2,N2-dimethylguanosine	1.709	13.780	eicosenoyl sphingomyelin	1.459	16.880
pyridoxine (Vitamin B6)	1.703	13.780	gulonic acid	1.453	16.880
sucrose	1.677	13.780	N-methyl proline	1.445	16.880
4-hydroxyhippurate	1.676	13.780	3-(4-hydroxyphenyl)propionate	1.402	16.880
2-aminoheptanoate	1.675	13.780	2-methylmalonyl carnitine	1.393	16.880
ribonate	1.670	13.780	dimethylmalonic acid	1.375	16.880
N-acetylneuraminate	1.670	13.780			

Supplementary Table 4. List of metabolites upregulated in IMH compared with IML older subjects. Compounds selected for experiments in primary monocytes are depicted in red.

Nature Medicine: doi:10.1038/nm.4267

	Antigen	Clone	Atomic Symbol	Atomic Mass	Vendor
SURFACE	Ter-119	TER-119	In	113	Biolegend/BD
	CD45	30-F11	In	115	Biolegend
	Ly6G	1A8	Pr	141	BD
	CD11b	M1/70	Nd	143	Fluidigm
	CD115	AFS98	Nd	144	Fluidigm
	CD4	RM4-5	Nd	145	Fluidigm
	CD8a	53-6.7	Nd	146	Fluidigm
	CD19	6D5	Sm	149	Fluidigm
	CD3	17A2	Sm	152	Fluidigm
	CD25	3C7	Gd	157	Fluidigm
	CD16	2.4G2	Gd	158	BD
	TCRγδ	GL3	Tb	159	Fluidigm
	CD62L	MEL-14	Gd	160	Fluidigm
	Ly6C	HK1.4	Dy	162	Fluidigm
	NK1.1	PK136	Ho	165	Fluidigm
	IgM	RMM-1	Er	169	Fluidigm
	CD49b	HMalpha2	Er	170	Fluidigm
	CD44	IM7	Yb	171	Fluidigm
	MHCII	M5/114.15.2	Yb	174	Fluidigm
	CD127	A7R34	Lu	175	BD
	B220	RA3-6B2	Lu	176	Fluidigm
INTRACELLULAR	pCREB	87G3/pS133	Nd	148	CST
	pSTAT5	47/pY694	Nd	150	Fluidigm
	pp38	36/p38/pT184/pY182	Eu	151	BD
	pSTAT1	4a/pY701	Eu	153	Fluidigm
	pSTAT3	4/P/pY705	Sm	154	BD
	prpS6	N7-548/pS235/236	Gd	155	Fluidigm
	Foxp3	NRRF-30	Gd	156	BD
	IκB	L35A5	Dy	164	Fluidigm
	NFκB	K10-895.12.50/pS529	Er	166	Fluidigm
	pERK1/2	D13.14.4E/pT202/Y404	Er	167	Fluidigm
	MAPKAPK2	27B7/pT334	Er	168	CST

Supplementary Table 5. Mouse Antibody Panel

Nature Medicine: doi:10.1038/nm.4267

Module 62

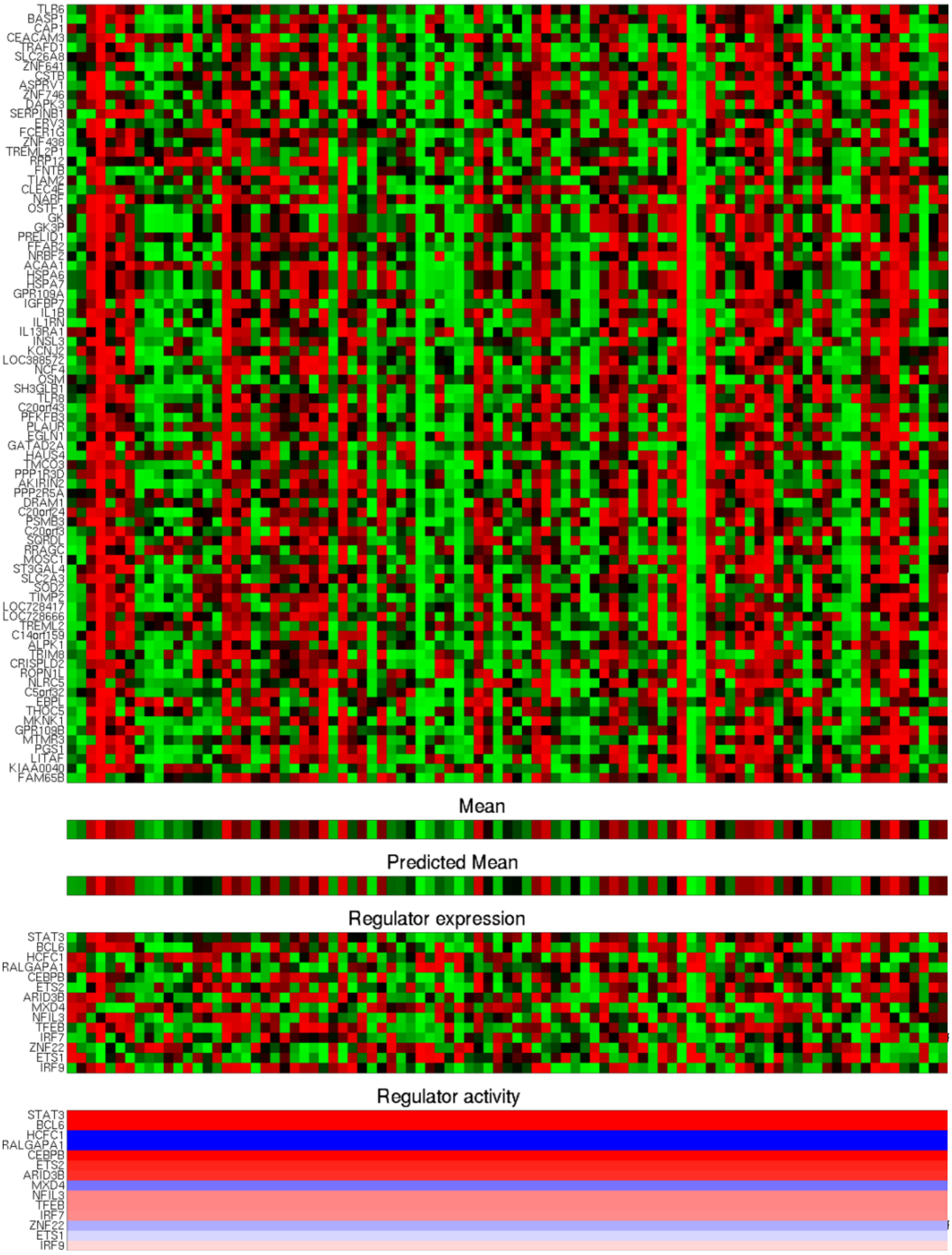

Nature Medicine: doi:10.1038/nm.4267

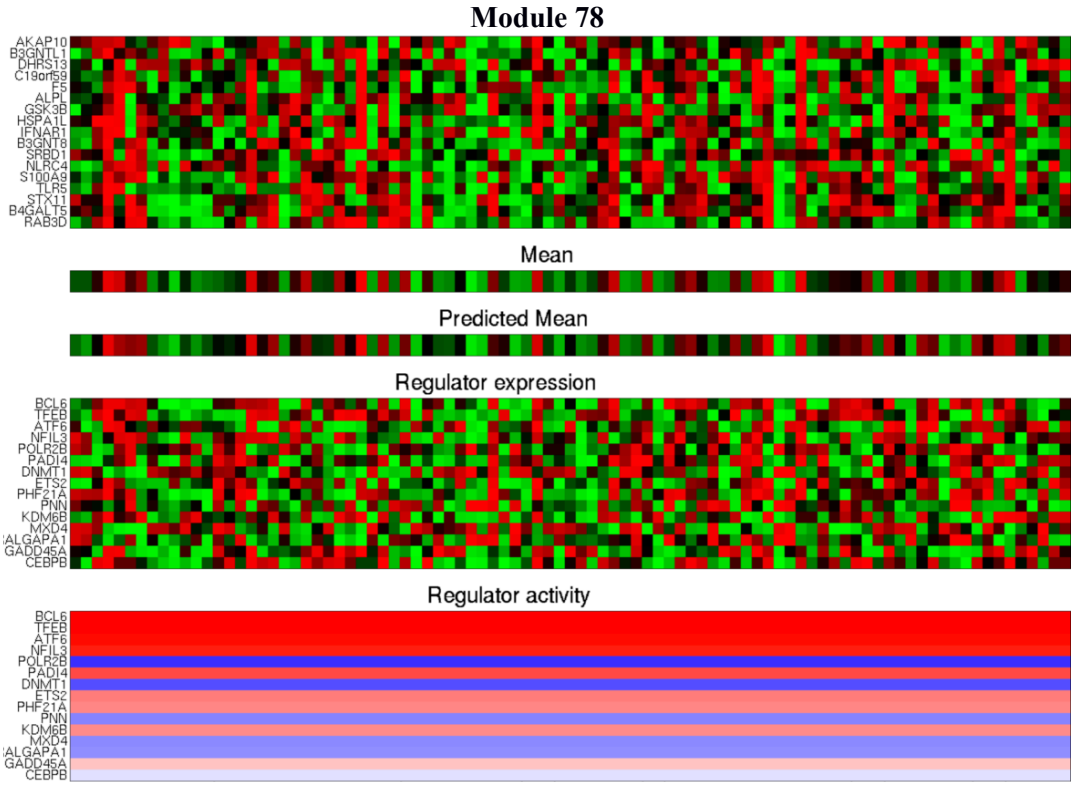

Figure S1. Age-associated modules containing genes related to inflammasome activity and regulation. Gene expression data from the Stanford-Ellison longitudinal cohort[1-3] was used to find changes in inflammasome-associated genes with age. Gene modules were derived from microarray data as previously described[2]. From a total of 41 age-associated gene modules (see also Fig. S2) only modules 62 (top) and 78 (bottom) were annotated to participate in cytokine production and both also show significant enrichment for inflammasome genes ($P < 0.01$).

Nature Medicine: doi:10.1038/nm.4267

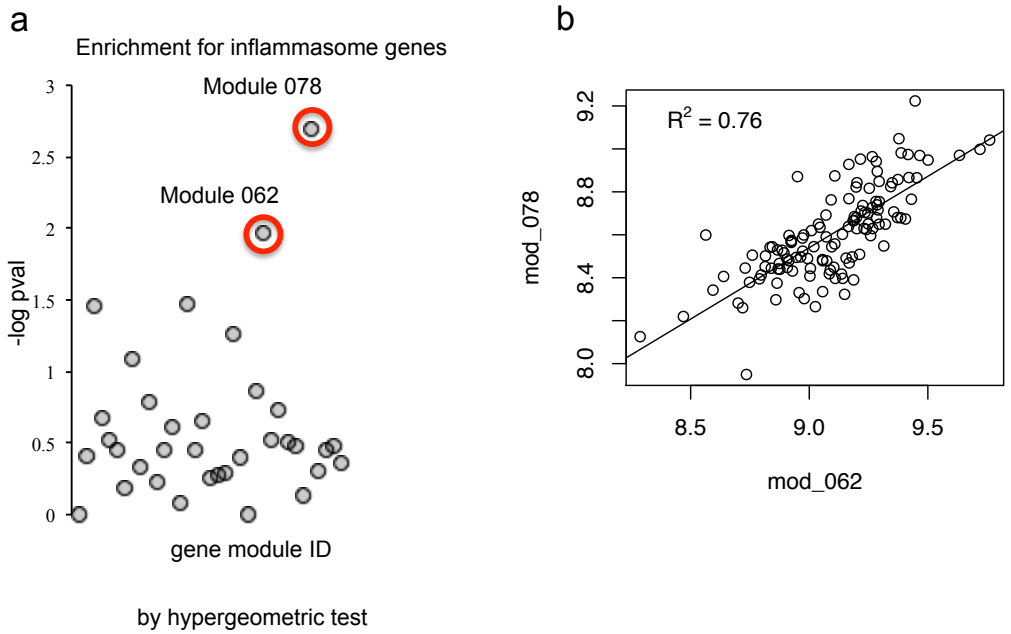

Figure S2. Modules 62 and 78 are enriched for inflammasome genes and their expression levels are highly correlated. (a) Enrichment analysis was conducted for 41 age-associated gene modules derived from the Stanford-Ellison longitudinal cohort[1-3] by hypergeometric test. Both gene modules 62 and 78 were significantly enriched for inflammasome genes ($P < 0.01$). Expression of gene modules 62 and 78 was highly correlated in individuals from the year 2008 data set (N = 89) ($P < 0.01$) (b).

Nature Medicine: doi:10.1038/nm.4267

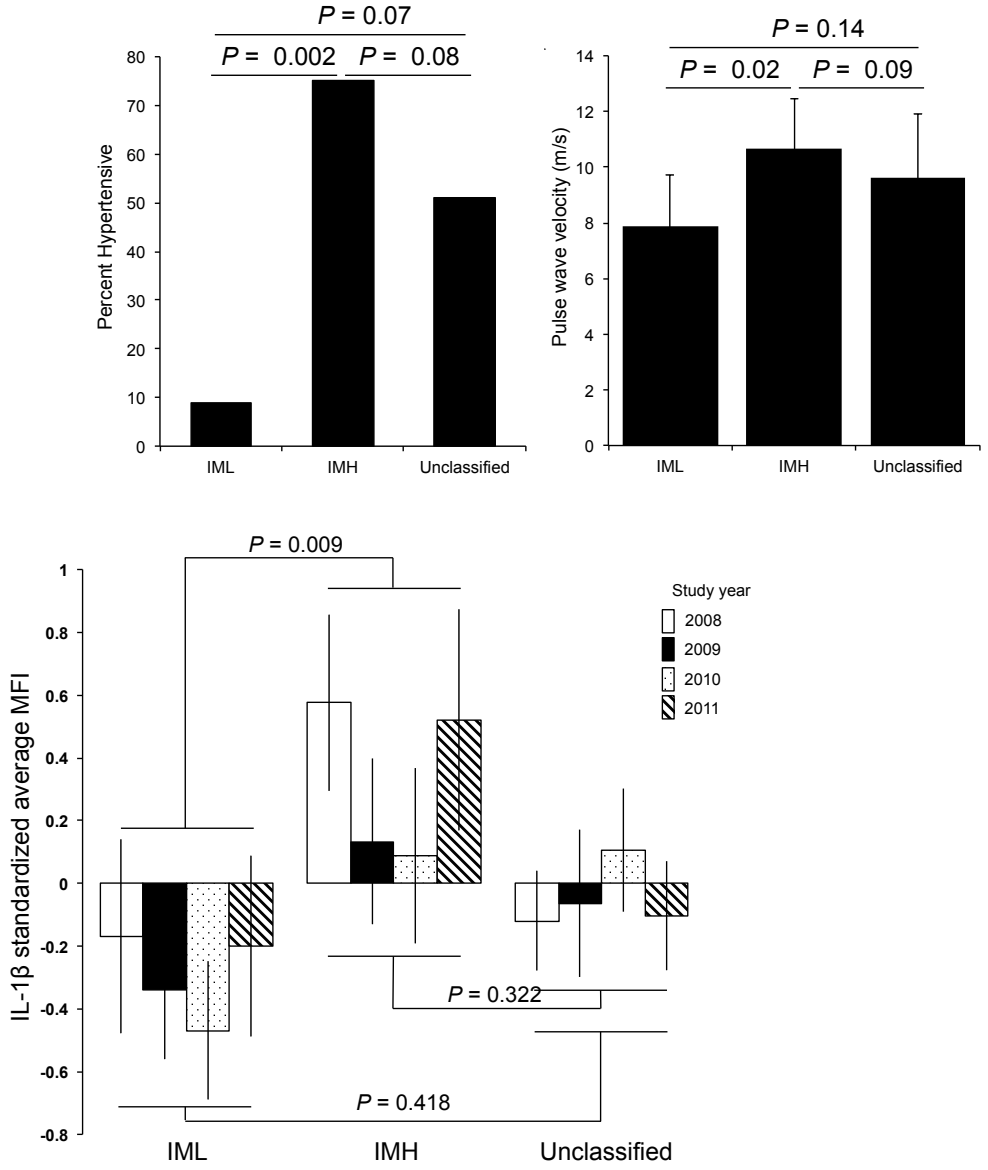

Figure S3. Hypertension rates, arterial stiffness and interleukin-1β levels in IML, IMH and unclassified older adults. Upper left: rates of hypertension in older IML, IMH and unclassified subjects shows that the extreme phenotypes IML and IMH are significantly different ($P = 0.002$ age-adjusted) and the unclassified group (intermediate phenotype) is not significantly different from either group. Upper right: pulse wave velocity in IML ($N = 8$), IMH ($N = 9$) and unclassified ($N = 22$) older adults shows significant differences between the IML and IMH groups (age-adjusted) but not in comparison with the group of unclassified older subjects. Bottom panel: the levels of IL-1β were analyzed from data collected during the years 2008 to 2011 in the IML group (N (2008, 2009, 2010, 2011) = 10, 10, 8, 7, respectively), IMH group (N (2008, 2009, 2010, 2011) = 12, 11, 12, 8, respectively) and unclassified older individuals (N (2008, 2009,

Nature Medicine: doi:10.1038/nm.4267

2010, 2011) = 39, 32, 31, 31, respectively). Significant differences are observed between the IML and IMH groups, but not between the IML group vs unclassified older adults nor between the IMH group vs unclassified older adults (age-adjusted) (left panel).

Nature Medicine: doi:10.1038/nm.4267

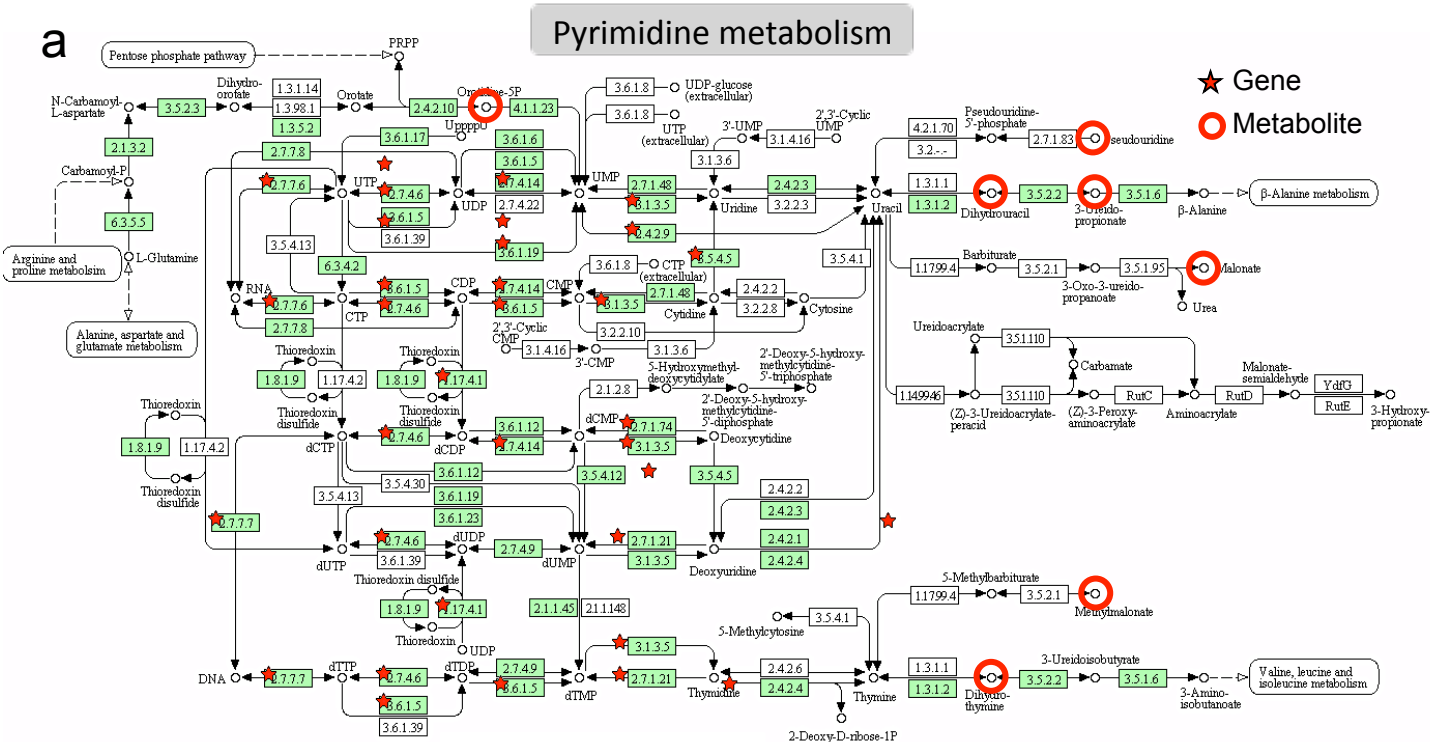

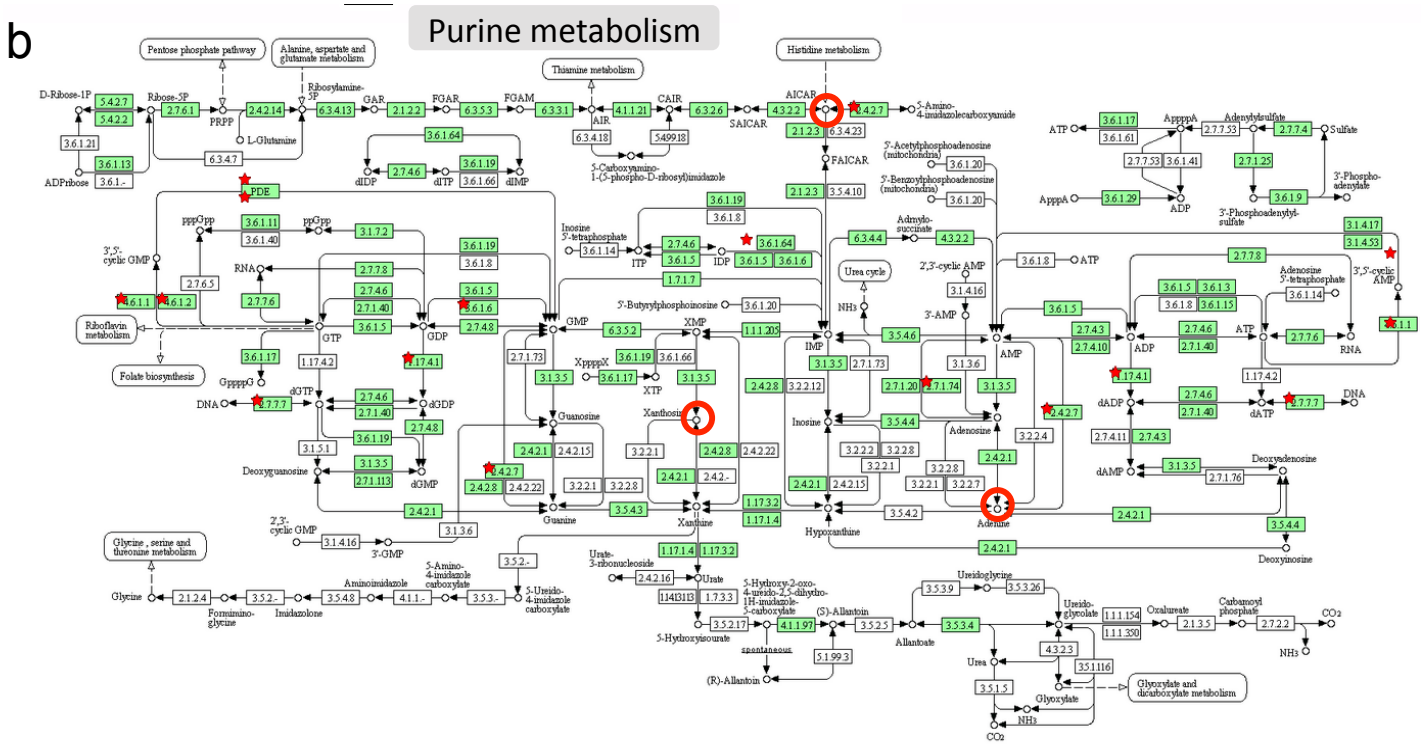

Nature Medicine: doi:10.1038/nm.4267

Figure S4. Pyrimidine and purine metabolism genes and metabolites differentially expressed in IML versus IMH individuals. Functional annotation and pathway analysis of a total of 67 differentially expressed metabolites (FDR $Q < 0.2$) was conducted using MetPA[16] and significant enrichment for pyrimidine metabolism (top) was identified with 7 compounds involved (a, red circles), as well as for purine metabolism (bottom) with 3 compounds involved (b, red circles) ($P < 0.05$ by hypergeometric test). A total of 104 pyrimidine metabolism genes (PYR) and 54 genes participating in purine metabolism (PUR) were gathered from KEGG[17]. Regression analysis was conducted on each gene's expression using microarray data from year 2008[1,2] against IML/IMH status (adjusted for age and sex) and significance for each regression coefficient was obtained via permutation tests[18]. PYR genes differentially expressed between IML and IMH included (the enzyme that a given gene encodes for is shown in parenthesis): POLR3E (2.7.7.6), POLD3 (2.7.7.7), NUDT2 (3.6.1.17), NME6 (2.7.4.6), ENTPD8 (3.6.1.5), CMPK2 (2.7.4.14), UMPK (2.7.4.22), ITPA (3.6.1.19), NT5E (3.1.3.5), UPRT (2.4.2.9), DCK (2.7.1.74), DCTD (3.5.4.12), TK1 (2.7.1.21), CDA (3.5.4.5), TYMP (2.4.2.4) and PNP (2.4.2.1) (a, red stars). PUR genes differentially expressed between IML and IMH included (the enzyme that a given gene encodes for is shown in parenthesis): ADCY1 (4.6.1.1), GUCY1A2 (4.6.1.2), PDE10A (PDE), PRUNE (3.6.1.11), POLD3 (2.7.7.7), RRM2B (1.17.4.1), CANT1 (3.6.1.6), APRT (2.4.2.7), NUDT16 (3.6.1.64), APRT (2.4.2.7) and PDE7B (3.1.4.53) (b, red stars). Genes differentially expressed were subjected to enrichment analysis by hypergeometric test. A significant enrichment is observed for both PYR and PUR pathways ($P < 0.05$ by hypergeometric test).

Nature Medicine: doi:10.1038/nm.4267

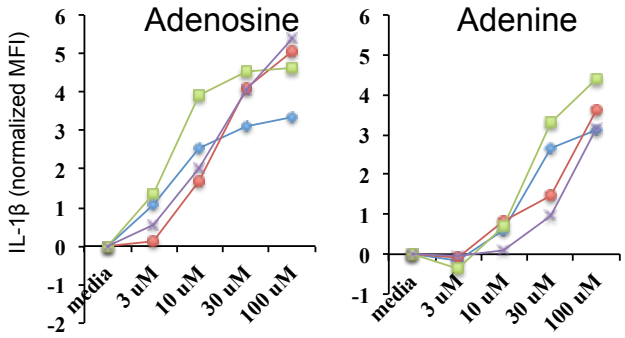

Figure S5. Dose-response experiments show dose-dependent increase in IL-1β with increasing concentrations of adenosine and adenine in human primary monocytes. Compounds were tested at increasing concentrations (0, 3, 10, 30, 100 μM) and displayed significant dose-responses ($P < 0.01$) in the concentration of cytokine found in the supernatants of treated monocytes from 4 healthy donors. To assess significance for the dose-response experiments we used Short Time-series Expression Miner (STEM)[19] which uses clustering methods for time-series or dose-response experiments and allows for the identification of significant dose-dependent profiles. $P < 0.01$ was considered statistically significant.

Nature Medicine: doi:10.1038/nm.4267

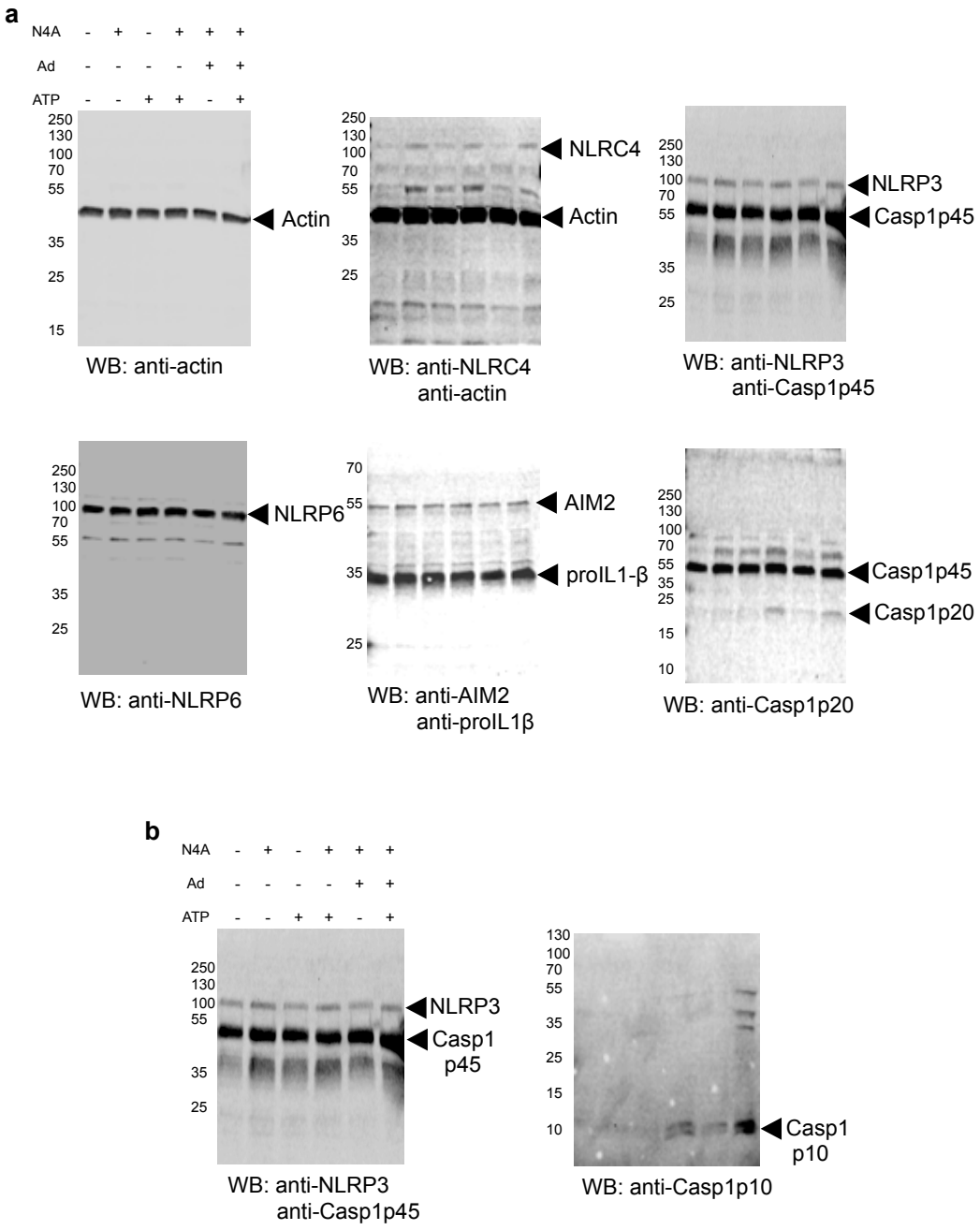

Figure S6. Metabolites in IMH individuals activate the NLRC4 inflammasome (a) Differentiated THP-1 cells were treated with compounds as indicated (1mM N4A; 300 μM adenine) for 6 hr or ATP 5 mM 30 min, cells were lysed and cell lysates were then immunoblotted with various antibodies to monitor expression of NLRs, Casp1, and proIL-1β. (b) Differentiated THP-1 cells were treated with compounds as before and cell lysates were submitted to immunoprecipitation with Biotinyl-YVAD-fmk peptide. Complexes were then recovered by using Streptavidin-sepharose beads and immunoblotted with anti-Caspase-1 p10 antibody.

Nature Medicine: doi:10.1038/nm.4267

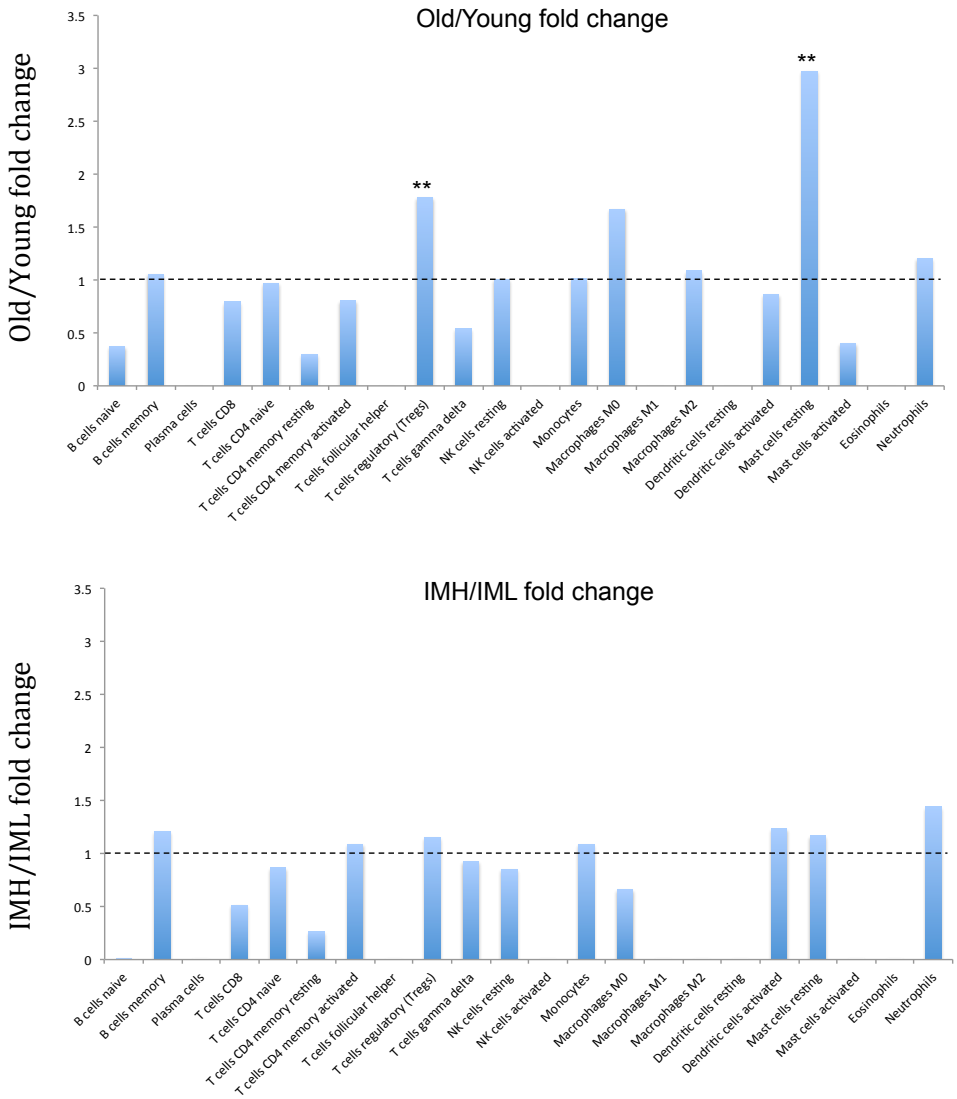

Figure S7. Cell subset frequencies estimates from whole blood in young and older adults, and in IMH versus IML older subjects. The frequencies of 22 different cell subsets were estimated based on whole-blood gene expression profiles in young and older adults ($N = 86$) (top panel) and in IMH and IML older adults ($N = 22$) (bottom panel). Significant differences in the estimated frequencies of circulating mast cells, as well as in the CD4 T regulatory cell compartment are observed between young and older adults ($P < 0.01$).

Nature Medicine: doi:10.1038/nm.4267

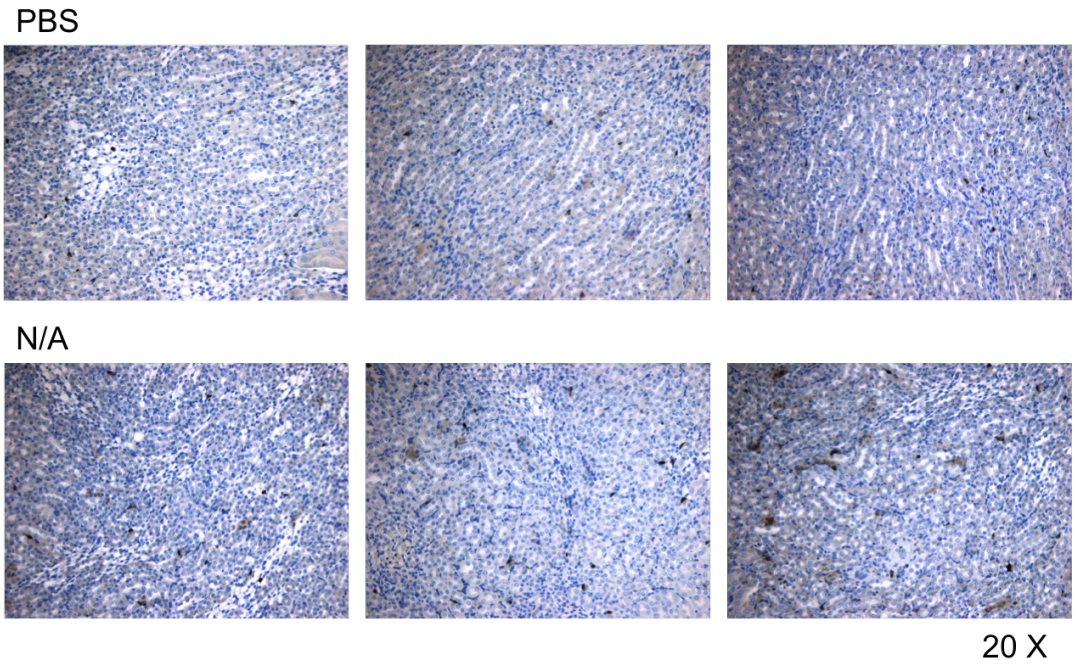

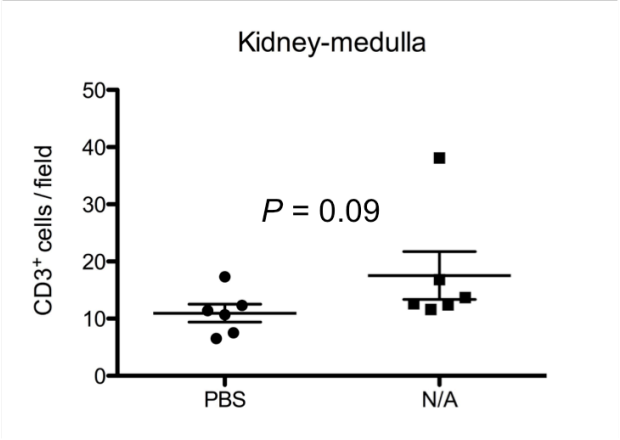

Figure S8. Kidney (medulla) sections from mice treated with N4A+Adenine show moderate infiltration of T cells. Mice were treated with N4A (N/A) (lower panel) or medium alone (upper panel) and sections of the kidney medulla were obtained and stained for CD3+ T cells. Eight fields per kidney (medulla region) were randomly chosen and CD3+ cells were counted. Kidneys from 6 mice were quantified per group. *P* corresponds to one-tail student *t*-test.

Nature Medicine: doi:10.1038/nm.4267

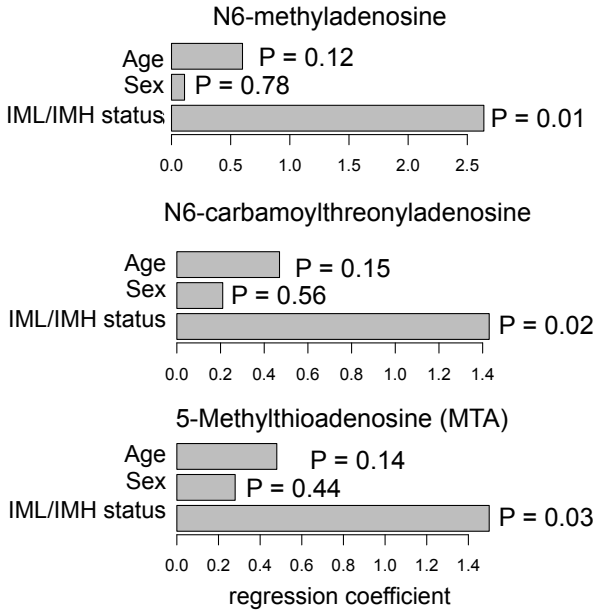

Figure S9. Adenosine derivatives are increased in IMH compared to IML subjects. The levels of adenosine and adenosine derivatives including N1-methyladenosine, N6-methyladenosine, N6-carbamoylthreonyladenosine, N6-succinyladenosine and 5-methylthioadenosine were compared between IMH ($N = 11$) and IML ($N = 9$) by multiple regression (adjusted for age and sex). Significant differences were found for N6-methyladenosine, N6-carbamoylthreonyladenosine 5-methylthioadenosine ($P < 0.05$). The bars represent the magnitude of regression coefficient from the fits.

Nature Medicine: doi:10.1038/nm.4267

Supplementary References

1. Furman, D.*, et al.* Systems analysis of sex differences reveals an immunosuppressive role for testosterone in the response to influenza vaccination. *Proceedings of the National Academy of Sciences of the United States of America* **111**, 869-874 (2014).
2. Furman, D.*, et al.* Apoptosis and other immune biomarkers predict influenza vaccine responsiveness. *Mol Syst Biol* **9**, 659 (2013).
3. Wang, C.*, et al.* Effects of aging, cytomegalovirus infection, and EBV infection on human B cell repertoires. *Journal of immunology* **192**, 603-611 (2014).
4. Jojic, V.*, et al.* Identification of transcriptional regulators in the mouse immune system. *Nature immunology* **14**, 633-643 (2013).
5. Segal, E.*, et al.* Module networks: identifying regulatory modules and their condition-specific regulators from gene expression data. *Nature genetics* **34**, 166-176 (2003).
6. Akaike, H. A new look at the statistical model identification. *IEEE Trans Auto Control* **19**, 716-723 (1974).
7. Subramanian, A.*, et al.* Gene set enrichment analysis: a knowledge-based approach for interpreting genome-wide expression profiles. *Proceedings of the National Academy of Sciences of the United States of America* **102**, 15545-15550 (2005).
8. Yaari, G., Bolen, C.R., Thakar, J. & Kleinstein, S.H. Quantitative set analysis for gene expression: a method to quantify gene set differential expression including gene-gene correlations. *Nucleic acids research* **41**, e170 (2013).
9. Newman, A.M.*, et al.* Robust enumeration of cell subsets from tissue expression profiles. *Nat Methods* **12**, 453-457 (2015).
10. Behbehani, G.K.*, et al.* Transient partial permeabilization with saponin enables cellular barcoding prior to surface marker staining. *Cytometry. Part A : the journal of the International Society for Analytical Cytology* (2014).
11. Gaudilliere, B.*, et al.* Implementing Mass Cytometry at the Bedside to Study the Immunological Basis of Human Diseases: Distinctive Immune Features in Patients with a History of Term or Preterm Birth. *Cytometry. Part A : the journal of the International Society for Analytical Cytology* **87**, 817-829 (2015).
12. Zunder, E.R.*, et al.* Palladium-based mass tag cell barcoding with a doublet-filtering scheme and single-cell deconvolution algorithm. *Nature protocols* **10**, 316-333 (2015).
13. Finck, R.*, et al.* Normalization of mass cytometry data with bead standards. *Cytometry. Part A : the journal of the International Society for Analytical Cytology* **83**, 483-494 (2013).
14. Benjamini, Y.H., Y. Controlling the False Discovery Rate: A Practical and Powerful Approach to Multiple Testing. *Journal of the Royal Statistical Society. Series B (Methodological)* **57**, 289-300 (1995).
15. Dai, H., Leeder, J.S. & Cui, Y. A modified generalized Fisher method for combining probabilities from dependent tests. *Frontiers in genetics* **5**, 32 (2014).

16. Xia, J. & Wishart, D.S. MetPA: a web-based metabolomics tool for pathway analysis and visualization. *Bioinformatics* **26**, 2342-2344 (2010).
17. Kanehisa, M.*, et al.* Data, information, knowledge and principle: back to metabolism in KEGG. *Nucleic acids research* **42**, D199-205 (2014).
18. Benjamini, Y. & Hochberg, Y. Controlling the false discovery rate: a practical and powerful approach to multiple testing. *J R Stat Soc* **B-57**, 289-300 (1995).
19. Ernst, J. & Bar-Joseph, Z. STEM: a tool for the analysis of short time series gene expression data. *BMC bioinformatics* **7**, 191 (2006).

Nature Medicine: doi:10.1038/nm.4267